

## Article

# Harnessing Symbiotic Mixotrophic Microalgal–Bacterial Biofilms for N and P Elimination

Mahshid Sedghi <sup>1,2,\*</sup> , John Fagan <sup>2</sup>, Soheil Sedghi <sup>3</sup>, Frithjof C. Küpper <sup>4,5,\*</sup>  and Ricardo Amils <sup>1</sup> 

<sup>1</sup> Centro de Biología Molecular Severo Ochoa (CSIC-UAM), Universidad Autónoma de Madrid, 28049 Madrid, Spain; ramils@cbm-csic.es

<sup>2</sup> R&D Department, ALGAESYS S.A., 2500-148 Caldas da Rainha, Portugal; john.fagan@algaesys.eu

<sup>3</sup> Department of Mechanical Engineering, Semnan Branch, Islamic Azad University, Semnan 3513137111, Iran; s\_sedghi@hotmail.com

<sup>4</sup> School of Biological Sciences, University of Aberdeen, Cruickshank Building, St Machar Drive, Aberdeen AB24 3UU, Scotland, UK

<sup>5</sup> Marine Biodiscovery Centre, Department of Chemistry, University of Aberdeen, Aberdeen AB24 3UE, Scotland, UK

\* Correspondence: sedghi.mahshid@hotmail.com (M.S.); fkuepper@abdn.ac.uk (F.C.K.); Tel.: +351-965065577 (M.S.)

**Abstract:** Symbiotic microalgal–bacterial biofilms can be very attractive for potato wastewater treatment. Microalgae remove nitrogen and phosphorus and simultaneously produce the oxygen that is required for the aerobic, heterotrophic degradation of organic pollutants. In this study, symbiotic microalgal–bacterial biofilms were grown in flow cells with ammonium and phosphate, and with acetate as a simulated biodegradable organic pollutant. The symbiotic biofilms removed acetate without an external oxygen or carbon dioxide supply, but ammonium and phosphate could not be completely removed. The biofilm was shown to have a considerable heterotrophic denitrification capacity. The symbiotic relationship between microalgae and aerobic heterotrophs was proven by subsequently removing light and acetate. In both cases, this resulted in the cessation of the symbiosis and in increasing effluent concentrations of both acetate and the nutrients ammonium and phosphate.

**Keywords:** mixotrophy; wastewater; nitrogen; phosphorus; wastewater treatment



**Citation:** Sedghi, M.; Fagan, J.; Sedghi, S.; Küpper, F.C.; Amils, R. Harnessing Symbiotic Mixotrophic Microalgal–Bacterial Biofilms for N and P Elimination. *Phycology* **2023**, *3*, 459–471. <https://doi.org/10.3390/phycolgy3040031>

Academic Editor: Marcin Dębowski

Received: 28 August 2023

Revised: 1 October 2023

Accepted: 3 October 2023

Published: 9 October 2023



**Copyright:** © 2023 by the authors. Licensee MDPI, Basel, Switzerland. This article is an open access article distributed under the terms and conditions of the Creative Commons Attribution (CC BY) license (<https://creativecommons.org/licenses/by/4.0/>).

## 1. Introduction

In wastewater treatment, the degradation of organic pollutants through heterotrophic microorganisms necessitates energy-intensive aeration for oxygen supply. However, the possibility of in situ oxygen production by microalgal species holds the potential to revolutionize the treatment process. This innovation could prove vital in the treatment of diverse wastewaters, including municipal, industrial, agro-industrial, and livestock effluents, driving more sustainable practices and even addressing the removal of toxic minerals [1]. Microalgal systems offer a multi-faceted solution by not only treating wastewater but also yielding oxygen and valuable bio-based ingredients for various applications. The efficient growth of microalgae in wastewater can significantly decrease production costs by capitalizing on the symbiotic relationship between wastewater and nutrient-rich microalgae. Moreover, incorporating microalgae-mediated CO<sub>2</sub> bio-mitigation into wastewater treatment infrastructures presents an economical and eco-friendly approach [2,3].

In this context, microalgal ponds have emerged as a promising platform where microalgae and bacteria collaborate symbiotically [4,5]. Bacteria enhance microalgal growth by producing auxins [6], and the reciprocal exchange of oxygen and carbon dioxide between microalgae and bacteria further amplifies the efficacy of the process [5,7]. Microalgal ponds effectively remove nitrogen and phosphorus via microbial growth and nitrification–denitrification processes [6,8–10].

One challenge lies in efficiently separating the microalgal–bacterial biomass from the treated wastewater. Innovations like the development of symbiotic microalgal–bacterial

biofilms offer a natural solution [11,12]. These biofilms enable the creation of a distinct boundary between the biomass and treated wastewater (Figure 1), thus facilitating the treatment process [13,14]. The potential of symbiotic microalgal–bacterial biofilms has been demonstrated in applications such as swine slurry treatment, where remarkable removal efficiencies of nitrogen, phosphorus, and chemical oxygen demand were achieved without an external oxygen supply [15–18].

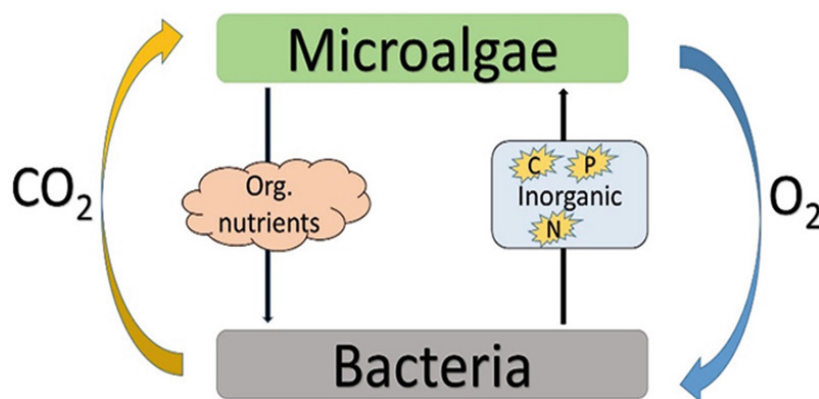


**Figure 1.** Schematic overview of symbiotic O<sub>2</sub> and CO<sub>2</sub> cycling in the biofilm.

To be a comprehensive wastewater treatment solution, symbiotic biofilms must target both organic pollutants and essential nutrients. By harnessing stoichiometric equations for microalgal growth and organic pollutant degradation, it is possible to design biofilms that thrive on wastewater with minimal external oxygen or CO<sub>2</sub> inputs. Such biofilms hold the potential to not only treat wastewater effectively but also remove residual nutrients, ensuring a comprehensive and sustainable treatment process [13,18–20].

This study focuses on establishing symbiotic microalgal–bacterial biofilms capable of efficiently consuming acetate, nitrogen, and phosphorus without an external oxygen supply in potato wastewater (PWW). Through rigorous monitoring and experimentation, this study investigates the viability of these biofilms and their potential contribution to PWW treatment efficiency. Moreover, the exploration of microalgal–bacterial interactions provides valuable insights into enhancing the sustainable management of wastewater resources. In general, PWW typically carries 350 mg of biodegradable COD/L, 50 mg of NH<sub>4</sub>-N/L, and 10 mg of PO<sub>4</sub><sup>3-</sup>-P/L. By employing stoichiometric equations for microalgal growth and aerobic degradation of organic pollutants, it is feasible that a microalgal–bacterial biofilm has the potential to thrive within this wastewater while effectively breaking down all the organic compounds without the need for external O<sub>2</sub> or CO<sub>2</sub> supplementation. In conclusion, the adoption of symbiotic microalgal–bacterial biofilms represent a transformative step towards more sustainable and efficient wastewater treatment. By harnessing the inherent capabilities of microalgae and bacteria, this innovative approach promises to address both organic pollutants and essential nutrients, contributing to a cleaner and more environmentally friendly future.

## 2. Materials and Methods

### 2.1. Experimental Setup

The experimental setup was composed of a dual-component system: a flow cell for synthetic wastewater inflow and a recycle vessel for effluent outflow, as depicted in Figure 2. Within the flow cell, a 1 mm PVC plastic sheet (0.018 m<sup>2</sup>) provided a substrate for the symbiotic biofilm, allowing a liquid layer of 2 cm to flow over it. Sensors positioned at the inflow and outflow of the flow cell continuously monitored the pH and dissolved oxygen (O<sub>2</sub>) concentration using InPro 6050/120 sensors from Mettler Toledo, Switzerland. The inflow pH was precisely maintained at 7.2 through controlled delivery of either acetate or a

blend of acetate and acetic acid (as detailed later). To maintain a consistent temperature of 23 °C, a water-jacketed glass tube facilitated the recycling of synthetic wastewater.

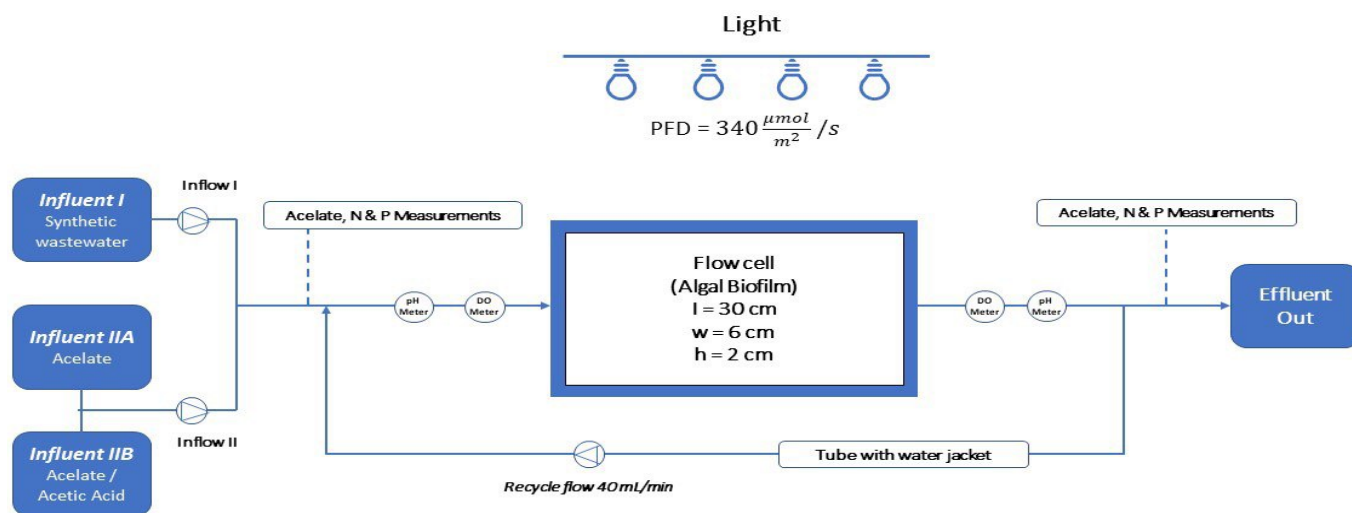


**Figure 2.** Schematic representation of the experiment setup.

To ensure constant illumination, fluorescent lamps (MASTER PL-L Polar 36W/840/4P, Philips, Amsterdam, The Netherlands) radiated light at an intensity as specified in Table 1. The chosen light intensities were determined based on the requirement to foster sufficient microalgal growth for the desired O<sub>2</sub> production level. In Experiment 1, a light intensity of 610 μmol/m<sup>2</sup>/s (inflow 3.4 mL/min) was employed, while Experiments 2, 3, and 4 adopted a light intensity of 340 μmol/m<sup>2</sup>/s (inflow 3 mL/min). The light intensity was meticulously gauged using a 2π PAR quantum sensor (SA190, LI-COR Biosciences, Lincoln, NE, USA) situated at the biofilm surface level.

**Table 1.** Experimental parameters and conditions.

Experiment	Influent I (mL/min)	Influent II (mL/min)	N in Synthetic Wastewater (mg/L)	N Loading Rate (g/m <sup>2</sup> /d)	HRT (h)	Extra HCO <sub>3</sub> <sup>-</sup>	Light Intensity (μmol/m <sup>2</sup> /s)
1	2.7	0.7	50	14	2.6	-	615
2	1.6	0.4	50	8	4.5	-	340
3	1.6	0.4	50	8	4.5	✓	340
4	1.6	0.4	50	8	4.5	✓	340

A series of succinct short-term assessments was conducted during the phase of stable acetate, nitrogen (N), and phosphorus (P) effluent concentrations. The details of these tests are outlined in Table 2. Test A encompassed the deactivation of the light supply. Experiment 4 incorporated air bubbling (Test B) to avert potential bacterial oxygen limitations. Test B necessitated replacing the water-jacketed tube of the setup with an aerated water-jacketed vessel. Test C focused on denitrification during Experiment 4, involving a third instance of light deactivation following the transition from NH<sub>4</sub><sup>+</sup> to NO<sub>3</sub><sup>-</sup> as the nitrogen source. Test D encompassed halting the acetate flow (influent II). This test was consistently conducted across all experiments, and in Experiments 2–4, the acetate flow was substituted with an equal flow of demineralized water.

**Table 2.** Settings of the four tests for symbiosis in the biofilm.

Test	Light	Acetate	Air	N Source	Experiment
A	X	✓	-	Ammonium	1, 2, 3, 4
B	X	✓	✓	Ammonium	4
C	X	✓	-	Nitrate	4
D	✓	X	-	Ammonium	1, 2, 3, 4

Note: ✓ stands for on and X stands for off.

## 2.2. Microalgal Biofilm Cultivation

Cultivation of *Chlorella vulgaris* BEA 0753B (*C. vulgaris*)

*C. vulgaris* (BEA 0753B), procured from the Culture Collection of Algae and Protozoa (The Spanish Bank of Algae—BEA), served as the microalgal strain for the study. Cultivation involved utilizing four PVC sheets (0.018 m<sup>2</sup>) placed within 250 mL Erlenmeyer flasks containing 100 mL of synthetic wastewater effluent.

The cultivation process unfolded in a controlled environment. The Erlenmeyer flasks were housed within an Innova 44 growth chamber (New Brunswick Scientific, Edison, NJ, USA), maintained at a temperature of 25 °C and subjected to orbital shaking at 100 rpm. Continuous illumination at 40 μmol photons/m<sup>2</sup>/s was achieved through fluorescent lamps. Additionally, a 2% CO<sub>2</sub> concentration was upheld in the gas phase. The culture was refreshed bi-weekly, involving the replacement of the synthetic wastewater effluent and the removal of the majority of microalgal biomass from the plastic sheet to facilitate re-growth and ensure culture viability.

A day before the commencement of the experiment, the flow cell's plastic sheet underwent sandpaper scratching and was subsequently coated with the cultivated microalgal biofilm, remaining immersed in synthetic wastewater for a minimum of 12 h. Approximately two hours prior to the experiment's initiation, approximately 20 mL of settled bacterial sludge was introduced onto the plastic sheet. For Experiments 1 and 2, this sludge originated from an aerobic membrane bioreactor operated at the Catalga Biotech S.L. laboratory (Vidreres, Spain). Notably, the bacteria used were acclimated to the specific cultivation conditions. In Experiment 4, the bacterial sludge was sourced from the aeration tank at Catalga Biotech, Spain, where nitrification occurred. For experimental consistency and reproducibility, a synthetic wastewater was utilized in place of real potato tuber wastewater. The synthetic wastewater, referred to as influent I, was composed to mimic potato wastewater. It contained N and P concentrations of 50 mg NO<sub>3</sub><sup>-</sup> N/L and 10 mg PO<sub>4</sub><sup>3-</sup> P/L, as well as other essential nutrients. The composition included NH<sub>4</sub>Cl, trace elements, vitamins, and additional nutrients based on Wright's cryptophyte medium [21]. Notably, Experiments 3 and 4 incorporated 1.05 g/L NaHCO<sub>3</sub> (10 mmol/L). The introduction of acetate, representative of biodegradable organic pollutants in typical potato wastewater, occurred at a concentration of 350 mg COD/L (323 mg acetate/L).

To ensure proper pH control, influent IIA and IIB were introduced separately to counteract pH fluctuations resulting from microbial growth. The N source was switched from NH<sub>4</sub><sup>+</sup> to NO<sub>3</sub><sup>-</sup> in Experiment 4, necessitating additional acetate inclusion to support denitrification. The adjustment aimed to ensure an adequate acetate supply for denitrification.

## 2.3. Analytical Procedures

Sampling from both influent and effluent flows during operation was carried out, with samples subsequently passed through a 0.45 μm filter (Millex-LCR, Merck Millipore, Jaffrey, NH, USA) for filtration. Colorimetric cuvette tests (LCK303, Hach Lange, Düsseldorf, Germany) were employed to analyse NH<sub>4</sub><sup>+</sup>-N concentrations. Ion chromatography (Compact IC 761 with a conductivity detector, Metrohm, Herisau, Switzerland) was utilized for the analysis of acetate, NO<sub>3</sub><sup>-</sup>-N, and PO<sub>4</sub><sup>3-</sup>-P concentrations [22].

To evaluate the yields of acetate, nitrate (NO<sub>3</sub><sup>-</sup>-N), and phosphate (PO<sub>4</sub><sup>3-</sup>-P) obtained under different operation conditions, ionic chromatography with a conductivity detector

was used. An anion-exchange column was used for the nitrate and phosphate analyses and a cation-exchange column for the acetate analysis. As a mobile phase, carbonate or bicarbonate were used as eluants for the nitrate and phosphate analyses and a cationic eluant for acetate. The flow rate was between 0.5 and 2.0 mL/min. The injection volume, between 5 and 100  $\mu$ L, was adjusted according to the sensitivity and the analyte concentration. A Metrohm conductivity detector (Switzerland) was configured according to Compact IC 761. Prepared calibration standards with known analyte concentration were used for calibration. QC checks using blanks and standards were implemented for quality control.

#### 2.4. Photosynthesis Inhibition and ROS Test

The biofilm biomass of Experiment 3 was subjected to incubation with acetate, generating microalgal suspensions with varying acetate concentrations: 0, 23, 123, 223, and 323 mg/L (as  $\text{NaC}_2\text{H}_3\text{O}_2 \cdot 3\text{H}_2\text{O}$ ) at an optical density of 0.2 at 680 nm. Following a 15 min period of darkness, the quantum yield was measured through the Aqua Pen C AP100's LC1 program (PSI, Drásov, Czech Republic) [19]. The release of hydrogen peroxide ( $\text{H}_2\text{O}_2$ ) into the water was used to assess reactive oxygen species (ROS) content. Hydrogen peroxide concentration in aqueous solution was determined using a colorimetric method employing phenolphthalein as an indicator [20].

#### 2.5. Biomass Separation and Characterization

Microalgae monitoring was conducted under a light microscope throughout the experiment. To segregate microalgae and bacteria based on density, the biomass of Experiment 3 underwent initial centrifugation at a low force of  $1000 \times g$  (Allegra X-12R, Beckman Coulter, Brea, CA, USA). This separation aimed to distinguish microalgae from the suspension. Subsequent centrifugation of the supernatant occurred at  $3273 \times g$  to differentiate the bacteria from the liquid. However, both microalgae and bacterial clusters settled after the initial centrifugation. In response, a solution containing 9 mmol EG-TA/g dry weight was formulated to dissolve extracellular polymeric substances, which held bacteria and microalgae together in clusters. The solution pH was adjusted to 10.2 using sodium hydroxide, followed by centrifugation as described earlier.

### 3. Results

#### 3.1. Biofilm Growth

The biofilm structure exhibited a relatively loose arrangement, necessitating weekly cleaning of the flow cell to prevent suspended growth. Visual observations of the harvested biofilm indicated that cohesive white clumps of biofilm persisted even after harvesting (Figure 3). Microscopic analysis revealed these clumps to be primarily composed of bacteria, likely bound together by extracellular polymeric substances (EPSs). Predominantly present in the biofilm were green microalgae from the genus *Chlorella*. A close inspection of the biofilm unveiled seasonal variations in species composition and dominance, including fluctuations involving cyanobacteria and a diatom, notably *Pseudoanabaena* sp. and *biofilm*. Moreover, the biofilm exhibited diverse phototrophic species, coexisting with the presence of numerous mosquito larvae. These dynamic interactions among species occasionally resulted in changes in the biofilm colouration. Single-cell microalgae and bacteria could typically be differentiated through centrifugation due to their differing weights. However, the clumps formed by microalgae and bacteria in these experiments posed difficulties in separation. To address this, the biomass from Experiment 3 underwent treatment with ethylene glycol-bis ( $\beta$ -aminoethyl ether)- $\text{N,N,N',N'}$ -tetraacetic acid (EGTA)—a chelating agent that eliminates calcium, an essential EPS component [23]. This treatment improved separation, indicating that EPSs likely played a role in holding bacterial clumps together. Despite these efforts, the measured bacterial fraction remained higher than the 11% recorded.

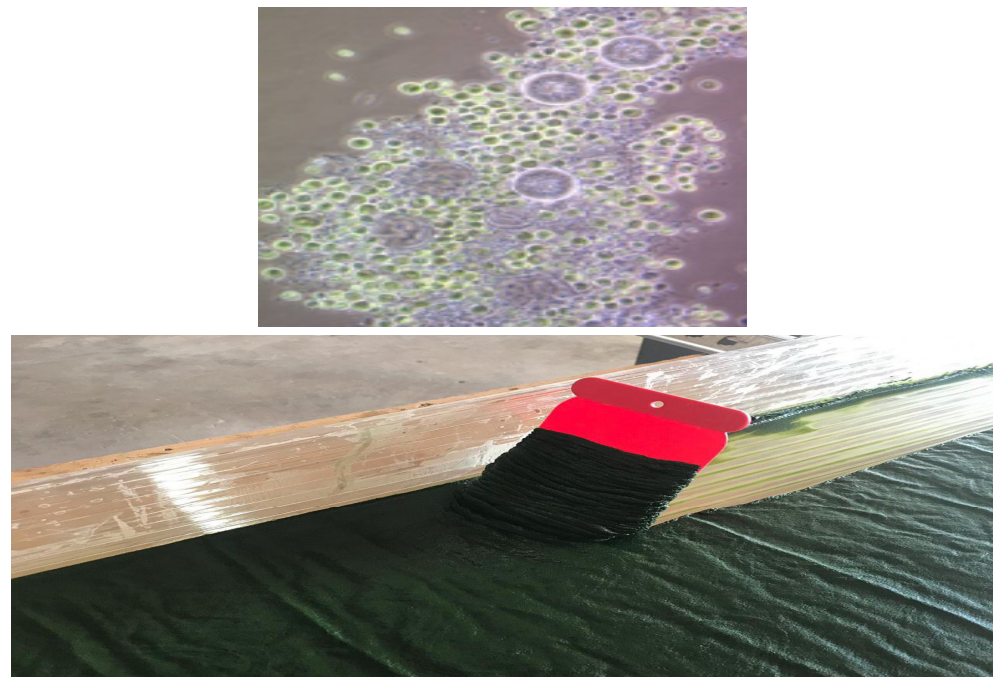


**Figure 3.** Micrographs of microalgal–bacterial interactions (*Chlorella vulgaris* biomass; **top**) and the symbiotic microalgal–bacterial biofilm (**bottom**).

### 3.2. Removal of Acetate, $\text{NO}_3^-$ , and $\text{PO}_4^{3-}$

Experiment 1 yielded a biofilm with microalgae and bacteria, but the concentrations of acetate,  $\text{NH}_4^+$ -N, and  $\text{PO}_4^{3-}$ -P in the effluent exceeded the anticipated values (Table 3), possibly due to the high light intensity causing photoinhibition. In Experiment 2, to mitigate this, the loading rates were reduced from 80 g acetate/ $\text{m}^2/\text{d}$ , 14 g N/ $\text{m}^2/\text{d}$ , and 2.7 g P/ $\text{m}^2/\text{d}$  to 50 g acetate/ $\text{m}^2/\text{d}$ , 8 g N/ $\text{m}^2/\text{d}$ , and 1.6 g P/ $\text{m}^2/\text{d}$ . Correspondingly, light intensity was lowered to 340  $\mu\text{mol}/\text{m}^2/\text{s}$ , resembling the average light intensity in Spain from late spring to early autumn. Despite these changes, acetate and  $\text{PO}_4^{3-}$ -P effluent concentrations remained elevated.

**Table 3.** The concentrations of ammonium and phosphate in the influent, the calculated effluent concentrations, and the average measured effluent concentrations of  $\text{NH}_4^+$ -N,  $\text{PO}_4^{3-}$ -P, and acetate in potato tuber waste.

	$\text{NH}_4^+$ -N (mg/L)	$\text{PO}_4^{3-}$ -P (mg/L)	Acetate (mg/L)
Influent	50	10	323
Effluent (calculated)	27	5.7	0
Experiment 1 Effluent	43	7.4	179
Experiment 2 Effluent	30	7.9	166
Experiment 3 Effluent	30	5.7	39

Experiment 3 explored the potential inhibition of the microalgal biomass by acetate at varying concentrations. The photochemical yield of photosystem II (PSII) was measured, and the results indicated that acetate did not inhibit photosynthesis within the tested concentrations (Figure 4). This ruled out acetate inhibition as the cause of the high effluent acetate levels in Experiments 1 and 2.

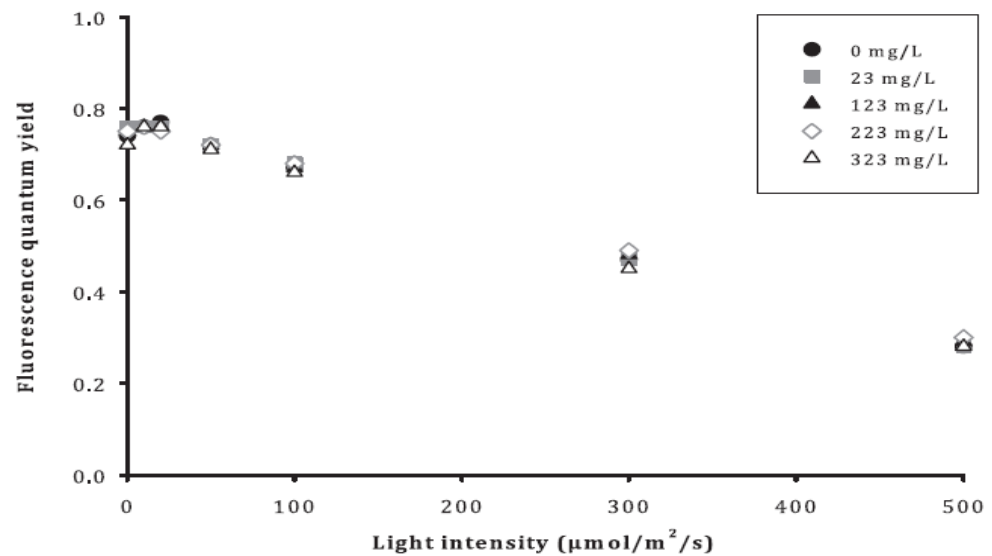


**Figure 4.** Adaptive photosynthetic resilience in response to variations in acetate concentration.

The biofilm in Experiment 3 was supplemented with bicarbonate ( $\text{HCO}_3^-$ ) to counter potential  $\text{CO}_2$  limitations, after which, acetate and  $\text{NH}_4^+$ -N concentrations rapidly decreased. The gradual reduction of  $\text{HCO}_3^-$  from day 16 to day 29 did not significantly impact acetate,  $\text{NH}_4^+$ -N, and  $\text{PO}_4^{3-}$ -P effluent concentrations. These concentrations remained comparable to the calculated values (Table 3)

Experiment 4 assessed the additional N removal through nitrification and denitrification. Despite inoculation with nitrifying sludge,  $\text{NH}_4^+$ -N and  $\text{NO}_3^-$ -N concentrations remained relatively stable. On day 18, the N source was switched from  $\text{NH}_4^+$  to  $\text{NO}_3^-$ , and the results demonstrated a significant N reduction along with acetate and  $\text{PO}_4^{3-}$ -P decreases (Figure 5).

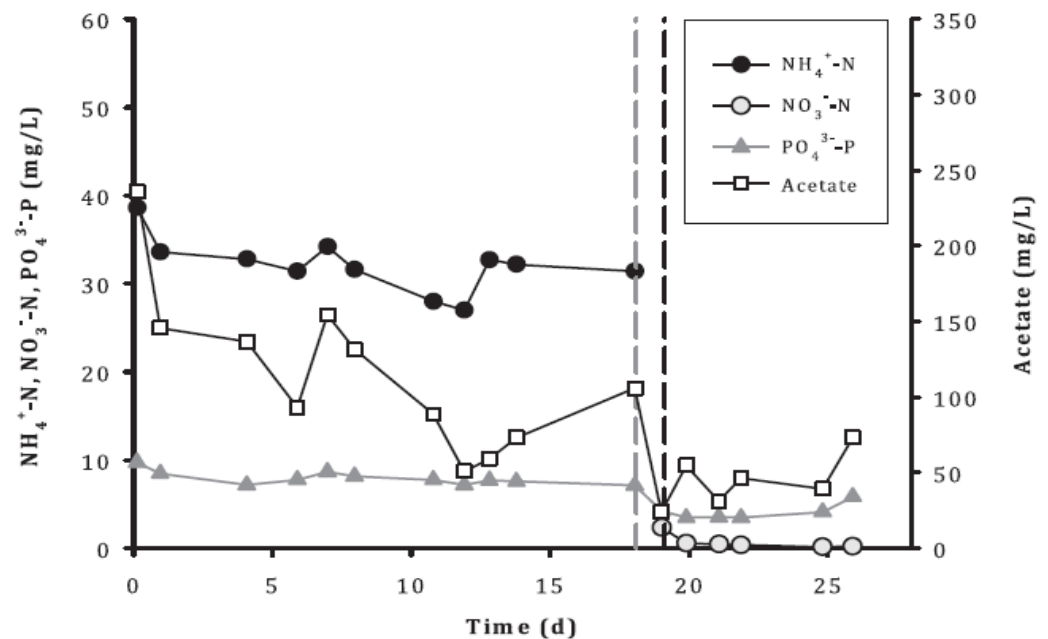


**Figure 5.** Nutrient and acetate dynamics in Experiment 4. The transition from  $\text{NH}_4^+$  to  $\text{NO}_3^-$  in the influent is represented by the grey dashed line, while the black dashed line signifies the rise in acetate concentration in the influent.

### 3.3. Symbiosis and ROS Test

Throughout all the experiments, the tests affirmed the symbiotic growth of microalgae and bacteria in the biofilm, with released hydrogen peroxide ( $\text{H}_2\text{O}_2$ ) serving as an ROS indicator in the effluent.

### 3.4. Darkness and Symbiosis

Tests conducted during Experiment 4 examined the biofilm responses in darkness. Test A, shown in Figure 6, revealed that effluent concentrations increased upon turning off the light, aligning with halted symbiotic growth.

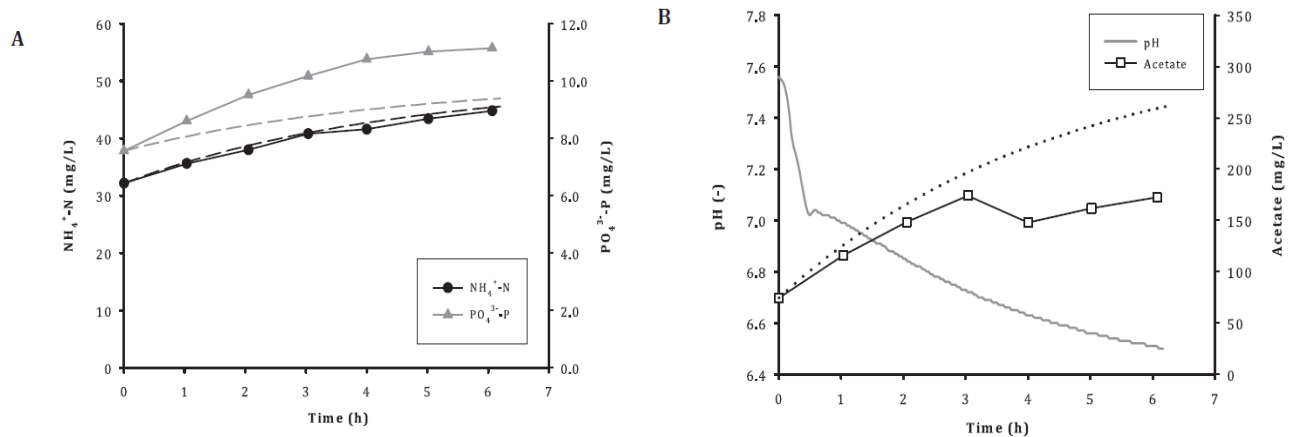


**Figure 6.** Nutrient and acetate responses after light deprivation. The theoretical increase in concentration of  $\text{NH}_4^+\text{-N}$ ,  $\text{PO}_4^{3-}\text{-P}$ , and acetate due to inflow dilutions is represented by black and grey dashed lines (A) and black dotted lines (B).

The experiment demonstrated the importance of microbial activity in maintaining effluent concentrations. Test B in Experiment 4 involved turning off the light while introducing air bubbling to maintain aerobic bacteria activity (Figure 7). This approach minimized nutrient uptake by bacteria, hinting at a predominant microalgal role in nutrient removal. In Test C of Experiment 4, the light was turned off after switching from  $\text{NH}_4^+$  to  $\text{NO}_3^-$  as the N source, evidencing bacterial denitrification (Figure 8).

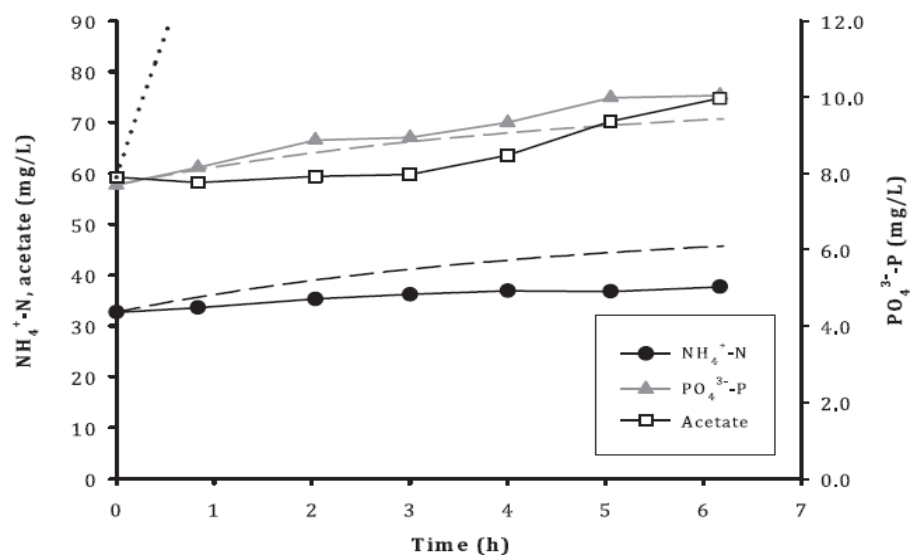


**Figure 7.** Nutrients and acetate responses under aeration after light deprivation. The black and grey dashed lines, along with the black dotted line, represent the theoretical increase in concentrations of  $\text{NH}_4^+\text{-N}$ ,  $\text{PO}_4^{3-}\text{-P}$ , and acetate resulting solely from inflow dilution.

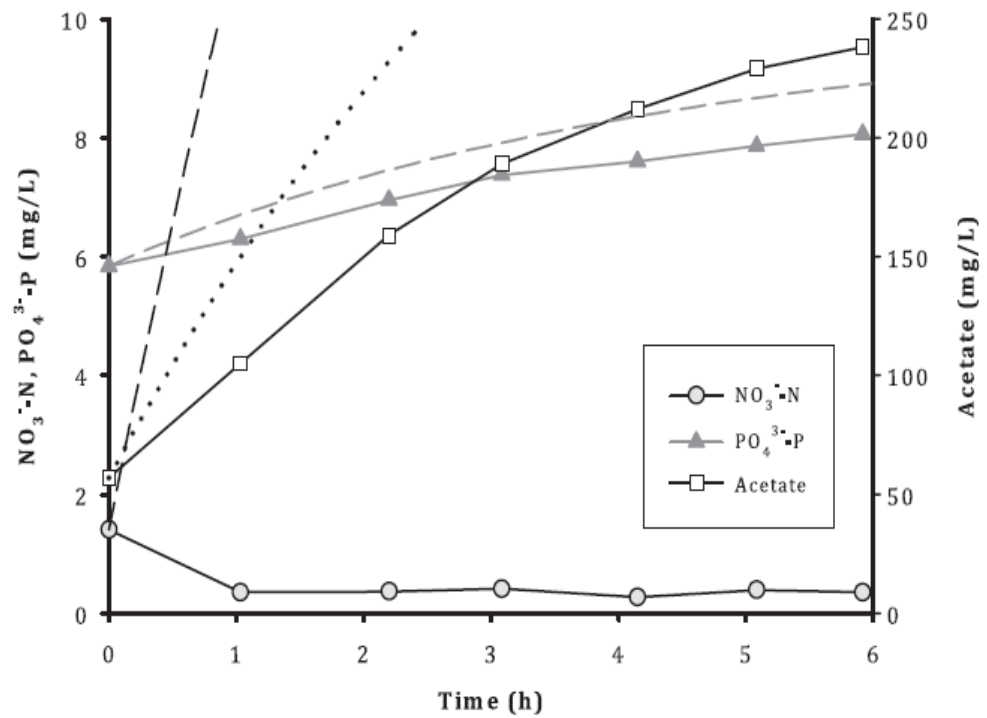


**Figure 8.** Effluent concentrations on NO<sup>3-</sup>-N, PO<sub>4</sub><sup>3-</sup>-P, and acetate under dark conditions (Test C). Theoretical increases in concentrations of NO<sup>3-</sup>-N, PO<sub>4</sub><sup>3-</sup>-P, and acetate resulting from inflow dilution are depicted by the black and grey dashed lines and the black dotted line.

### 3.5. Acetate Depletion and Symbiosis

Test D in Experiment 4 investigated acetate depletion by stopping its addition. The biofilm exhibited sustained microalgal activity, possibly supported by excess CO<sub>2</sub> production. This led to further growth, suggesting that acetate-independent CO<sub>2</sub> sustenance promoted microalgal activity even without acetate addition (Figure 9).

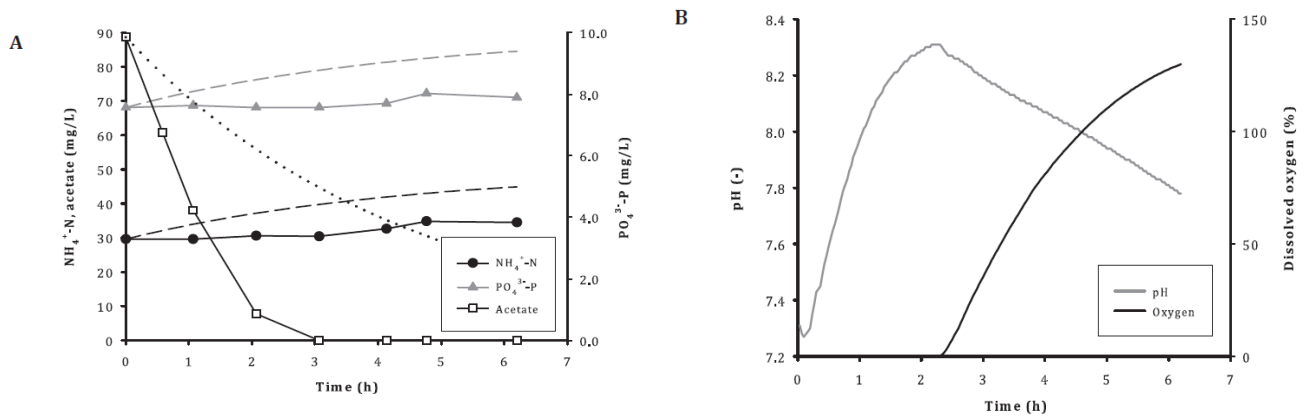


**Figure 9.** pH/dissolved oxygen levels (B) in effluent after acetate addition was turned off (Test D). The black and grey dashed lines, along with the black dotted lines marked as (A), illustrate the theoretical rise in NH<sub>4</sub><sup>+</sup>-N, PO<sub>4</sub><sup>3-</sup>-P, and acetate concentrations (A) due solely to inflow dilution.

## 4. Discussion

The findings of this study showcase the successful cultivation of a symbiotic microalgal-bacterial biofilm without the need for external oxygen and carbon dioxide supply. However, the establishment of the symbiotic relationship necessitated the addition of bicarbonate (HCO<sub>3</sub><sup>-</sup>) during the biofilm start-up phase. Moreover, fluorescence measurements of chlorophyll indicated that microalgal growth remained unhampered by acetate concentrations of

up to 323 mg/L. This value is slightly above the concentration of 295 mg/L but below the inhibitory range exceeding 400 mg/L, as reported in previous studies [12,24].

The symbiotic biofilm displayed removal efficiencies of 3.2 g  $\text{NH}_4^+\text{-N}/\text{m}^2/\text{d}$ , 0.41 g  $\text{PO}_4^{3-}\text{-P}/\text{m}^2/\text{d}$ , and 43 g  $\text{COD}/\text{m}^2/\text{d}$ , surpassing the removal rates of 1.0 g  $\text{NO}_3^-\text{-N}/\text{m}^2/\text{d}$  and 0.13 g  $\text{PO}_4^{3-}\text{-P}/\text{m}^2/\text{d}$  achieved in a previous flow cell-based microalgal biofilm study [25]. It is important to note that the comparison of these removal rates might not be entirely straightforward, given the varying objectives of the studies. While the previous study aimed for extremely low effluent nutrient concentrations, the current study did not achieve such low levels. The effective elimination of acetate was observed, although the symbiotic biofilm could not completely remove all  $\text{NH}_4^+$  and  $\text{PO}_4^{3-}$ . The insufficiency of light and  $\text{CO}_2$  hindered microalgal uptake of these residual nutrients. As such, if symbiotic biofilms are considered for wastewater treatment, additional nutrient removal methods might be required. Such augmentation could be achieved through increased microalgal growth via enhanced light and  $\text{CO}_2$  supplementation. The light intensity used in this study was akin to the average light intensity of 30 mol/m<sup>2</sup>/d found in Spain during late spring to early autumn [26], indicating that tropical climates might be more conducive for such symbiotic biofilm systems.

Enhanced nitrogen (N) removal can be accomplished through nitrification and denitrification. Previous studies have suggested the feasibility of nitrification and denitrification within biofilms in pond systems [9,25] and photobioreactors [27]. However, the symbiotic system may lack the necessary oxygen surplus [25]. Alternatively, additional phosphorus (P) removal can be achieved through calcium or magnesium phosphate precipitation due to the pH elevation within the biofilm [28]. Our study on symbiotic microalgal–bacterial biofilms complement the findings from the acetate-focussed study by offering a practical application of biofilm technology for wastewater treatment, while the Raunkjer et al. study contributes to our understanding of how biofilms respond to changing conditions. Together, we can emphasize the potential of biofilm-based systems in addressing various challenges in wastewater treatment and highlight the need for further research in this dynamic field [29].

Although the biofilm of Experiment 4 was introduced to nitrifying sludge, no nitrification was detected, which could be attributed to low biofilm  $\text{O}_2$  concentrations, as evidenced by the 0% dissolved  $\text{O}_2$  content of the effluent. Nitrification dependency on  $\text{O}_2$  levels in the bulk phase, as seen in microalgal pond biofilms [5,6], could explain the absence of measurable nitrification. Furthermore, the short 1-day inoculation process and the 19-day growth period might have led to inadequate nitrifier colonization. Prior research used a three-week inoculation period to establish a mixed microalgal and nitrifying culture [27]. Nonetheless, the presence of nitrifying populations within microalgal–bacterial biofilms submerged in microalgal ponds [4,30] suggests that nitrification within symbiotic biofilms is achievable.

In Experiment 4, transitioning from  $\text{NH}_4^+$  to  $\text{NO}_3^-$  as the nitrogen source demonstrated the denitrification capacity of the biofilm. This shift led to substantial  $\text{NO}_3^-$  removal from the wastewater. The prominence of denitrification over microalgal assimilation is indicated by the preference of  $\text{NH}_4^+$  over  $\text{NO}_3^-$  as a nitrogen source [11]. The swift  $\text{NO}_3^-$  reduction implies the presence of denitrifiers in biofilm niches with low  $\text{O}_2$  concentrations. This transition suggests that denitrifiers within the biofilm could switch from  $\text{O}_2$  to  $\text{NO}_3^-$  as an electron acceptor upon  $\text{NO}_3^-$  introduction [10,31]. The COD consumption of 5.9 g  $\text{COD}/\text{g NO}_3^-\text{-N}$  upon light deactivation is consistent with expectations for heterotrophic denitrification. It is worth noting that effective bacterial denitrification in biofilms has historically faced challenges due to limited bulk liquid–biomass contact surface area, a critical factor for treatment effectiveness, especially in comparison to suspended growth systems [18].

For the practical implementation of symbiotic biofilms in wastewater treatment, several factors need consideration. Firstly, biodegradable particles entrapped in the biofilm may be hydrolysed and removed, potentially necessitating a pre- or post-treatment step.

Pre-treatment could result in a lower COD supply and subsequently lower heterotroph CO<sub>2</sub> production. Consequently, additional CO<sub>2</sub> would need supplementation to sustain microalgal growth. Secondly, since microalgae remain photosynthetically inactive during the night, symbiotic biofilms could be used to complement wastewater treatment. Lastly, while microalgal biomasses offer potential benefits, separating microalgae from bacteria remains a challenge. Thus, finding appropriate applications for the mixed biomass is vital. The biomass might serve as fertilizer if devoid of heavy metals or recalcitrant compounds. Alternatively, the biomass could become feedstock for biogas production via anaerobic digestion, but would require post-treatment for autotrophic N and P removal.

## 5. Conclusions

This study conclusively demonstrates the feasibility of cultivating a symbiotic microalgal–bacterial biofilm capable of effectively removing acetate, ammonium, and phosphate from potato wastewater. Impressive removal rates of 3.2 g NH<sub>4</sub><sup>+</sup>-N/m<sup>2</sup>/d, 0.41 g PO<sub>4</sub><sup>3-</sup>-P/m<sup>2</sup>/d, and 43 g COD/m<sup>2</sup>/d were achieved. The establishment of the symbiotic relationship between microalgae and bacteria was achieved by introducing additional HCO<sub>3</sub><sup>-</sup> during the experiment's outset. Remarkably, a subsequent external supply of oxygen or carbon dioxide was unnecessary. The symbiotic nature of the bacteria and microalgae within the biofilm was substantiated by the temporary cessation of light or acetate supply. Moreover, the present findings imply that nitrogen removal could potentially be expanded by enhancing light and CO<sub>2</sub> availability and/or utilizing nitrification and denitrification processes. The swift establishment of denitrifying bacteria within the symbiotic biofilm highlights its potential for future applications. In essence, this research underscores the viability of symbiotic biofilms as a proficient mechanism for wastewater treatment.

## 6. Patents

ALGAESYS S.A. has a License of the patent, which is registered under IP EP3907195A1.

**Author Contributions:** M.S.: R&D Director/Investigator, Writing—original draft. J.F.: Founder and CEO, Writing—original draft. S.S.: Mechanical engineer, Design, Writing—review and editing. F.C.K.: Supervision, Writing—review and editing. R.A.: Supervision, Conceptualization, Methodology, Writing—review and editing. All authors have read and agreed to the published version of the manuscript.

**Funding:** This research was funded by Catalga Biotech. S.L., ALGAESYS S.A., and FCK received support from the Marine Alliance for Science and Technology for Scotland pooling initiative. MASTS is funded by the Scottish Funding Council (grant reference HR09011) and contributing institutions.

**Institutional Review Board Statement:** Not applicable.

**Informed Consent Statement:** Not applicable.

**Data Availability Statement:** Data will be made available on request. The following supporting information can be downloaded at: [https://patentscope.wipo.int/search/en/detail.jsf?docId=EP341188107&\\_cid=P12-LJ41HO-07571-1](https://patentscope.wipo.int/search/en/detail.jsf?docId=EP341188107&_cid=P12-LJ41HO-07571-1) (accessed on 28 August 2023), WIPO—Search International and National Patent Collections.

**Acknowledgments:** The authors extend their gratitude to their colleagues at Catalga Biotech for generously providing all the necessary equipment.

**Conflicts of Interest:** The authors declare no conflict of interest.

## References

1. Abdel-Raouf, N.; Al-Homaidan, A.A.; Ibraheem, I.B.M. Microalgae and wastewater treatment. *Saudi J. Biol. Sci.* **2012**, *19*, 257–275. [[CrossRef](#)]
2. Kuo, C.M.; Jian, J.F.; Lin, T.H.; Chang, Y.B.; Wan, X.H.; Lai, J.T.; Chang, J.S.; Lin, C.S. Simultaneous microalgal biomass production and CO<sub>2</sub> fixation by cultivating *Chlorella* sp. GD with aquaculture wastewater and boiler flue gas. *Bioresour. Technol.* **2016**, *221*, 241–250. [[CrossRef](#)]

3. Collotta, M.; Champagne, P.; Mabee, W.; Tomasoni, G. Wastewater and waste CO<sub>2</sub> for sustainable biofuels from microalgae. *Algal Res.* **2018**, *29*, 12–21. [[CrossRef](#)]
4. De-Bashan, L.E.; Bashan, Y. Joint immobilization of plant growth-promoting bacteria and green microalgae in alginate beads as an experimental model for studying plant-bacterium interactions. *Appl. Environ. Microbiol.* **2008**, *74*, 6797–6802. [[CrossRef](#)]
5. Babu, M.; Hes, E.; van der Steen, N.; Hooijmans, C.; Gijzen, H. Nitrification rates of algal–bacterial biofilms in wastewater stabilization ponds under light and dark conditions. *Ecol. Eng.* **2010**, *36*, 1741–1746. [[CrossRef](#)]
6. Craggs, R.J.; Tanner, C.C.; Sukias, J.P.; Davies-Colley, R.J. Nitrification potential of attached biofilms in dairy farm waste stabilisation ponds. *Water Sci. Technol.* **2000**, *42*, 195–202. [[CrossRef](#)]
7. Higgins, P.G.; Prior, K.; Harmsen, D.; Seifert, H. Development and evaluation of a core genome multilocus typing scheme for whole-genome sequence-based typing of *Acinetobacter baumannii*. *PLoS ONE* **2017**, *12*, e0179228. [[CrossRef](#)]
8. Kim, K.; Han, J.-I. Performance of direct alkaline sulfide fuel cell without sulfur deposition on anode. *Int. J. Hydrog. Energy* **2014**, *39*, 7142–7146. [[CrossRef](#)]
9. Babu, M.A.; van der Steen, N.P.; Hooijmans, C.M.; Gijzen, H.J. Nitrogen mass balances for pilot-scale biofilm stabilization ponds under tropical conditions. *Bioresour. Technol.* **2011**, *102*, 3754–3760. [[CrossRef](#)]
10. Johnson, L.M.; Smith, R.J.; Thompson, K.W.; Chen, H.; Lee, S. Characterization of Anoxic Microniches and Microbial Processes in Aerated Activated Sludge. *Environ. Sci. Technol.* **2023**, *58*, 3025–3032.
11. Gupta, A.; Lee, S.M.; Kim, D.; Park, J. Synergistic Effects of Marine Bacteria on Microalgal Growth: Insights into a Balanced Inorganic/Organic Carbon Ratio. *J. Appl. Phycol.* **2023**, *35*, 87–95.
12. Xue, F.; Miao, C.; Ma, Y.; Shi, M.; Zheng, H.; Chen, F.; Ye, N. Effects of Organic Carbon Sources on Growth, Photosynthesis, and Respiration of *Phaeodactylum tricornutum*. *Biotechnol. Bioeng.* **2016**, *113*, 536–545.
13. Boelee, N.C.; Temmink, H.; Janssen, M.; Buisman, C.J.N.; Wijffels, R.H. Scenario Analysis of Nutrient Removal from Municipal Wastewater by Microalgal Biofilms. *Water* **2012**, *4*, 460–473. [[CrossRef](#)]
14. Pikula, K.; Zakharenko, A.; Aruoja, V.; Golokhvast, K.; Tsatsakis, A. Oxidative stress and its biomarkers in microalgal ecotoxicology. *Curr. Opin. Toxicol.* **2019**, *13*, 8–15. [[CrossRef](#)]
15. De Godos, I.; González, C.; Becares, E.; García-Encina, P.; Muñoz, R. Simultaneous Nutrients and Carbon Removal During Pretreated Swine Slurry Degradation in a Tubular Biofilm Photobioreactor. *Appl. Microbiol. Biotechnol.* **2009**, *82*, 187–194. [[CrossRef](#)]
16. Holmes, D.E.; Dang, Y.; Smith, J.A. Nitrogen cycling during wastewater treatment. In *Advances in Applied Microbiology*; Elsevier: Amsterdam, The Netherlands, 2019; Volume 106. [[CrossRef](#)]
17. González, C.; Marciniak, J.; Villaverde, S.; León, C.; García, P.A.; Muñoz, R. Efficient Nutrient Removal from Swine Manure in a Tubular Biofilm Photo-Bioreactor Using Algae-Bacteria Consortia. *Water Sci. Technol.* **2008**, *58*, 95–102. [[CrossRef](#)]
18. Tchobanoglous, G.L.; Burton, F.; Stensel, D.H. *Metcalf & Eddy: Wastewater Engineering: Treatment and Reuse*; McGraw Hill Companies: New York, NY, USA, 2014; Issue 7.
19. Flaming, I.A.; Kromkamp, J. Light dependence of quantum yields for PSII charge separation and oxygen evolution in eucaryotic algae. *Limnol. Oceanogr.* **1998**, *43*, 284–297. [[CrossRef](#)]
20. Smith, J.K.; Johnson, A.B.; Williams, C.D. Kinetics of Hydrogen Peroxide Decomposition in High-Temperature Water. *J. Radioanal. Nucl. Chem.* **2023**, *185*, 213–220.
21. Andersen, R.A.; Berges, J.A.; Harirson, P.J.; Watanabe, M.M. Appendix A—Recipes for Freshwater and Seawater Media. In *Algal Culturing Techniques*; Elsevier: Amsterdam, The Netherlands, 2005.
22. Duboc, P.; Marison, I.; von Stockar, U. Quantitative Calorimetry and Biochemical Engineering. In *Handbook of Thermal Analysis and Calorimetry*; Kemp, R.B., Ed.; Elsevier: Amsterdam, The Netherlands, 1999; Volume 4, pp. 287–309. [[CrossRef](#)]
23. Smith, J.K.; Johnson, A.B.; Thompson, K.W.; Chen, H.; Lee, S. Impact of Ethylene Glycol-Bis (B-Aminoethyl Ether)-N, N-Tetraacetic Acid (EGTA) on Methanogenic Granular Sludge: Stability and Activity Analysis. *Environ. Sci. Technol.* **2023**, *45*, 3210–3217.
24. Bouarab, L.; Dauta, A.; Loudiki, M. Heterotrophic and mixotrophic growth of *Micractinium pusillum* Fresenius in the presence of acetate and glucose: Effect of light and acetate gradient concentration. *Water Res.* **2004**, *38*, 2706–2712. [[CrossRef](#)]
25. Boelee, N.C.; Temmink, H.; Janssen, M.; Buisman, C.J.N.; Wijffels, R.H. Nitrogen and phosphorus removal from municipal wastewater effluent using microalgal biofilms. *Water Res.* **2011**, *45*, 5925–5933. [[CrossRef](#)] [[PubMed](#)]
26. Huld, T.A.; Sári, M.; Dunlop, E.D.; Albuissou, M.; Wald, L. Integration of HELIOCLIM-1 Database Into PV-GIS to Estimate Solar Electricity Potential in Africa. In Proceedings of the 20th European Photovoltaic Solar Energy Conference and Exhibition, Barcelona, Spain, 6–10 June 2005.
27. Karya, N.G.N.I.; van der Steen, N.P.; Lens, P.N.L. Photo-oxygenation to support nitrification in an algal–bacterial consortium treating artificial wastewater. *Bioresour. Technol.* **2013**, *134*, 244–250. [[CrossRef](#)] [[PubMed](#)]
28. Roeselers, G.; van Loosdrecht, M.C.M.; Muyzer, G. Phototrophic biofilms and their potential applications. *J. Appl. Phycol.* **2008**, *20*, 227–235. [[CrossRef](#)] [[PubMed](#)]
29. Raunkjær, K.; Nielsen, P.H.; Hvitved-Jacobsen, T. Acetate removal in sewer biofilms under aerobic conditions. *Water Res.* **1997**, *31*, 2727–2736. [[CrossRef](#)]

30. McLean, B.M.; Baskaran, K.; Connor, M.A. The use of algal-bacterial biofilms to enhance nitrification rates in lagoons: Experience under laboratory and pilot-scale conditions. *Water Sci. Technol.* **2000**, *42*, 187–194. [[CrossRef](#)]
31. Anderson, J.M.; Smith, R.L.; Thompson, K.W.; Chen, H.; Lee, S. Long-Term Persistence of Bacterial Denitrification Capacity under Aerobic Conditions. *J. Environ. Microbiol.* **2023**, *25*, 523–530.

**Disclaimer/Publisher’s Note:** The statements, opinions and data contained in all publications are solely those of the individual author(s) and contributor(s) and not of MDPI and/or the editor(s). MDPI and/or the editor(s) disclaim responsibility for any injury to people or property resulting from any ideas, methods, instructions or products referred to in the content.